Legend for Supplementary Figures:

Figure S1: Equal expression of constructs used in Figure 1B. HeLa cells were transfected with FLAG-tag plasmids encoding p50RhoGAP, PGAP, NBCH or ΔPRR and their expression levels were verified by Western blot analyses for the whole cell lysates (WCL) with anti-FLAG, and normalized with the expression levels of endogenous tubulin as the loading control.

Figure S2: Quantitative analyses of p50RhoGAP, NBCH, and PGAP expression levels in cells. HeLa cells were transfected with FLAG-tag plasmids expressing p50RhoGAP, PGAP or NBCH, fixed and subjected to confocal fluorescence microscopy as described in 'Materials and Methods'. The expressed proteins were detected by indirect immunostaining with Alexa Fluor 633-dye-conjugated goat anti-rabbit IgG against anti-FLAG. Intensity of signal detected by confocal microscopy was employed to determine the relative protein expression levels across various regions of cell populations as indicated by the lines and arrows. Briefly, images were collected using a Zeiss 510 Meta laser-scanning microscope equipped with a 60X len. The detector gain was first optimized by sampling various regions of the coverslip and then fixed for each specified channel. Once set, the detector gain value was kept constant throughout the image acquisition process. As a result, signal intensities from identical channels of different images could be used for quantitative measurements.

Figure S3: The BCH domains of BNIP-Sα and p50RhoGAP display distinct cellular effects and distributions. HeLa cells were transfected with plasmids encoding FLAG-tagged BCH domain of BNIP-Sα. Cells were then fixed and subjected to confocal fluorescence microscopy as described in 'Materials and Methods'. Morphological changes and cytoskeletal rearrangements

were revealed by indirect immunostaining with anti-tubulin for microtubules, followed by Alexa Fluor 488-dye-conjugated goat anti-mouse IgG. White arrows indicate rounding cells that expressed BCH domain of BNIP-Sα while the yellow arrows in the enlarged inset figure indicate their distinct punctate structures.

Figure S4: Quantitative analysis of RBD assay. For quantitative analysis, the bands of three independent RBD studies were scanned and analyzed with image J software. The densitometry ratios of p50RhoGAP, NBCH or PGAP with RhoA alone were calculated. Data are means ± s.d. (n=3). Differences between values not sharing the same letters (a, b, c) are statistically significant at p<0.01.

Figure S5: The PGAP triple-point mutant R282A/R283A/N391V lost its effect on RhoA-induced stress fiber formation. HeLa cells were transfected with plasmids encoding HA-PGAP wildtype or mutants (R282A, N391V, R282A/R283A, R282A/N391V, R282A/R283A/N391V) in the presence of FLAG-RhoA. Cells were then fixed and subjected to confocal fluorescence microscopy as described in 'Materials and Methods'. The actin-filaments were detected by direct staining with rhodamine-conjugated phalloidin.

Figure S6: The endosomal localization of p50RhoGAPdoes not required for regulating GAP activity. (A) GFP- or FLAG-tagged p50RhoGAP were co-transfected with markers such as red fluorescent protein-endoplasmic reticulum (RFP-ER) (Clontech), GPI-green fluorescent protein (GFP) or lysosomal-associated membrane protein (Lamp1)-GFP. Cells were then fixed after 16-20 hours and subjected to confocal fluorescence microscopy as described in 'Materials and

Methods'. Mitochondria were stained with MitoTracker Orange CMTMRos (Invitrogen) according to manufacturer's instructions. For monitoring endosomal localization, HeLa cells on coverslips were incubated in extracellular H-medium (145 mM NaCl, 5 mM KCl, 1 mM $MgCl_2$, 0.8 mM $CaCl_2$, 10 mM HEPES, 5 mM glucose, pH 7.4) for 20 min at 37 °C, then medium was replaced with H-medium containing 10 μg/ml Alexa568-transferrin (Invitrogen) for 20 minutes followed by fixation and confocal microscopy analysis. (B) HeLa cells were transfected for 16-20 hours with FLAG-tagged-SNX-PGAP or PGAP mutants. Cells were then fixed and incubated with FLAG monoclonal antibodies, followed by Alexa Fluor 488-dye-conjugated goat anti-mouse IgG. (C) HeLa cells were transfected for 16-20 hours with FLAG-tagged-SNX-PGAP mutant. Cells were then fixed and incubated with mouse anti-EEA1 for endosome or FLAG polyclonal antibody for SNX-PGAP, followed by Alexa Fluor 488-dye-conjugated goat anti-mouse IgG or by Alexa Fluor 568-dye-conjugated goat anti-rabbit IgG, respectively.

Figure S7: BCH domain from S. pombe could not functionally substitute the BCH domain of p50RhoGAP. (A) Sequence alignments of BCH domains from *H. sapiens* p50RhoGAP/Cdc42GAP (Q07960) and *S. pombe* GTPase-activating protein (NM_001018711) using ClustalW and formatted using BOXSHADE. Identical residues are shaded black whereas similar or conserved residues are in gray. The BCH and GAP domain were indicated by box whereas conserved R282 arginine finger, R283 arginine residue and N391 mutated and used in earlier experiment (Fig. 2E) were indicated by the asterisks. (B) HeLa cells were transfected with FLAG-tagged p50RhoGAP or with a hybrid mutant where the BCH domain was replaced by the *pombe*-BCH domain. Cells were then fixed and incubated with FLAG monoclonal antibodies, followed by Alexa Fluor 488-dye-conjugated goat anti-mouse IgG. Cell morphology was

monitored by direct staining with rhodamine-conjugated phalloidin for actin filaments. (C) Cells co-transfected with HA-tagged RhoA and FLAG-pBCHhPG or FLAG-p50RhoGAP were immunoprecipitated (IP) with anti-FLAG beads. The bound RhoA was detected by anti-HA (first panel), and equal loading of IP beads were verified by anti-FLAG (second panel). Expression of FLAG-tagged and HA-tagged proteins were verified by Western blot analyses of the whole cell lysates (wcl) using anti-FLAG (third panel) and anti-HA (bottom panel), respectively. (D) To determine the impact of pBCHhGAP in regulating RhoA activity inside the cells, HeLa cells were transfected with HA-tagged RhoA in the presence and absence of FLAG-tagged pBCHhGAP. Cell were lysed and incubated with GST fusion of the Rho-binding domain of rhotekin immobilized on beads, as described under 'Materials and Methods.' Bound RhoA were resolved on SDS–PAGE and detected by immunoblotting with HA-antibody (first panel). Equal loading of GST fusion proteins is shown in the second panel.

Figure S8: The non-RhoA binding NBCH mutants still retained their ability to form homophilic interaction. Cells were co-transfected with HA-tagged NBCH and FLAG-tagged NBCH wild-type or mutants as depicted in Figure 5B. Lysates were immunoprecipitated (IP) with anti-FLAG beads. The bound NBCH was detected by anti-HA (third panel), and equal loading of IP beads were verified by anti-FLAG (bottom panel). Protein expression were verified by Western blot analyses of the whole cell lysates (wcl) using anti-FLAG (first panel) and anti-HA (second panel), respectively.

Figure S9: The equal expression of constructs used in Figure 7A. HeLa cells were transfected with FLAG-tagged plasmids for p50RhoGAP, FLBCH, FL121, FL161, FL181 or PGAP.

Expression of these plasmids was verified by Western blot analyses of the whole cell lysates (wcl) using anti-FLAG and compared with the expression levels of tubulin as the loading control.

Figure S10: Quantitative analysis of the expression of p50RhoGAP mutants in cells. HeLa cells were transfected with FLAG-tagged plasmids used in Figure 7A. Cells were then fixed followed by indirect immunostaining with Alexa Fluor 633-dye-conjugated goat anti-rabbit IgG against anti-FLAG. Intensity of signal detected by confocal microscopy was employed to determine the relative protein expression levels across various regions of cell populations as indicated by the lines and arrows. Briefly, images were collected using a Zeiss 510 Meta laser-scanning microscope equipped with a 60X len. The detector gain was first optimized by sampling various regions of the coverslip and then fixed for each specified channel. Once set, the detector gain value was kept constant throughout the image acquisition process. As a result, signal intensities from identical channels of different images could be used for quantitative measurements.

Figure S11: p50RhoGAP knockdown cells still display normal actin cytoskeleton network. (A) HEK293T cells were transfected with different constructs of pSilencer2.1-U6 hygro plasmids for p50RhoGAP (see below), and screened for clones that either failed to knockdown (#1) or conferring successful knockdown (#3) by analyzing the expression of Flag-tagged p50RhoGAP as the target. (B) HeLa cells were co-transfected for 20 hours 1 μg pSilencer2.1-U6 hygro plasmids for p50RhoGAP and 0.3 μg GFP vector as the tracer/marker to indicate transfected cells. Cytoskeletal networks were revealed by direct staining with rhodamine-conjugated

phalloidin for actin filaments and cell borders. The short hairpin RNA (shRNA) oligonucleotides against human p50RhoGAP were kind gifts from Robert R. Krauss (Mount Sinai School of Medicine). The shRNA sequences are:

p50RhoGAP#1: (5′-3′)

GATCCCGGCCAAGCTCTGAACCAGTTTTCAAGAGAAACTGGTTCAGAGCTTGGCTTT TTTGGAAA;

p50RhoGAP#3: (5′-3′)

GATCCCGCCATCACCCTCAAGGCTATTTCAAGAGAATATAGCCTTGAGGGTGATGGT TTTTTGGAAA.

Figure S12: p50RhoGAP interacts with p115RhoGEF via its BCH domain. HEK293T cells were transfected with plasmid encoding myc-p115RhoGEF alone or with FLAG-p50RhoGAP, NBCH or PGAP. Lysates were immunoprecipitated (IP) with anti-FLAG beads, and the associated proteins detected with myc antibody (first panel). Expression of FLAG-tagged proteins and HA-RhoA were verified by Western blot analyses by anti-FLAG (third panel) and anti-myc (bottom panel), respectively. Equal loading of IP beads were verified by anti-FLAG (second panel).

Figure S1

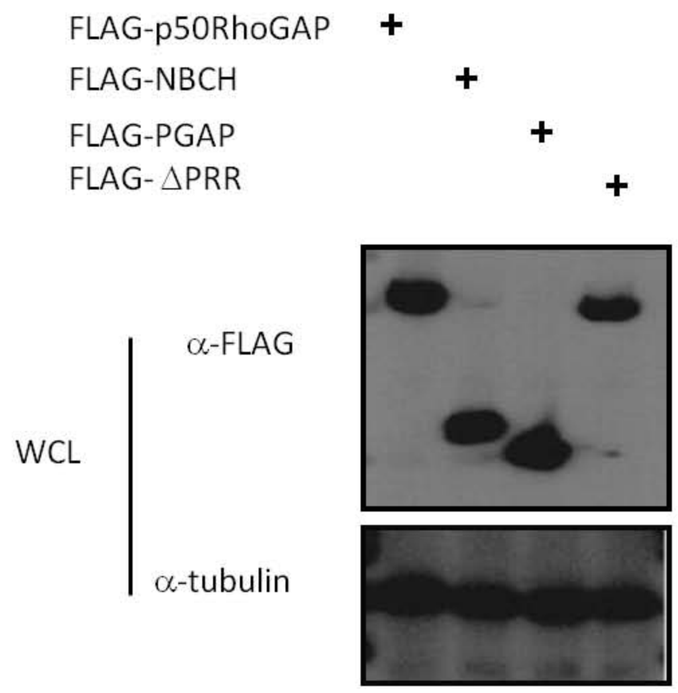
FLAG-p50RhoGAP +
FLAG-NBCH +
FLAG-PGAP +
FLAG- ΔPRR +
WCL
α-FLAG
α-tubulin

Figure S2

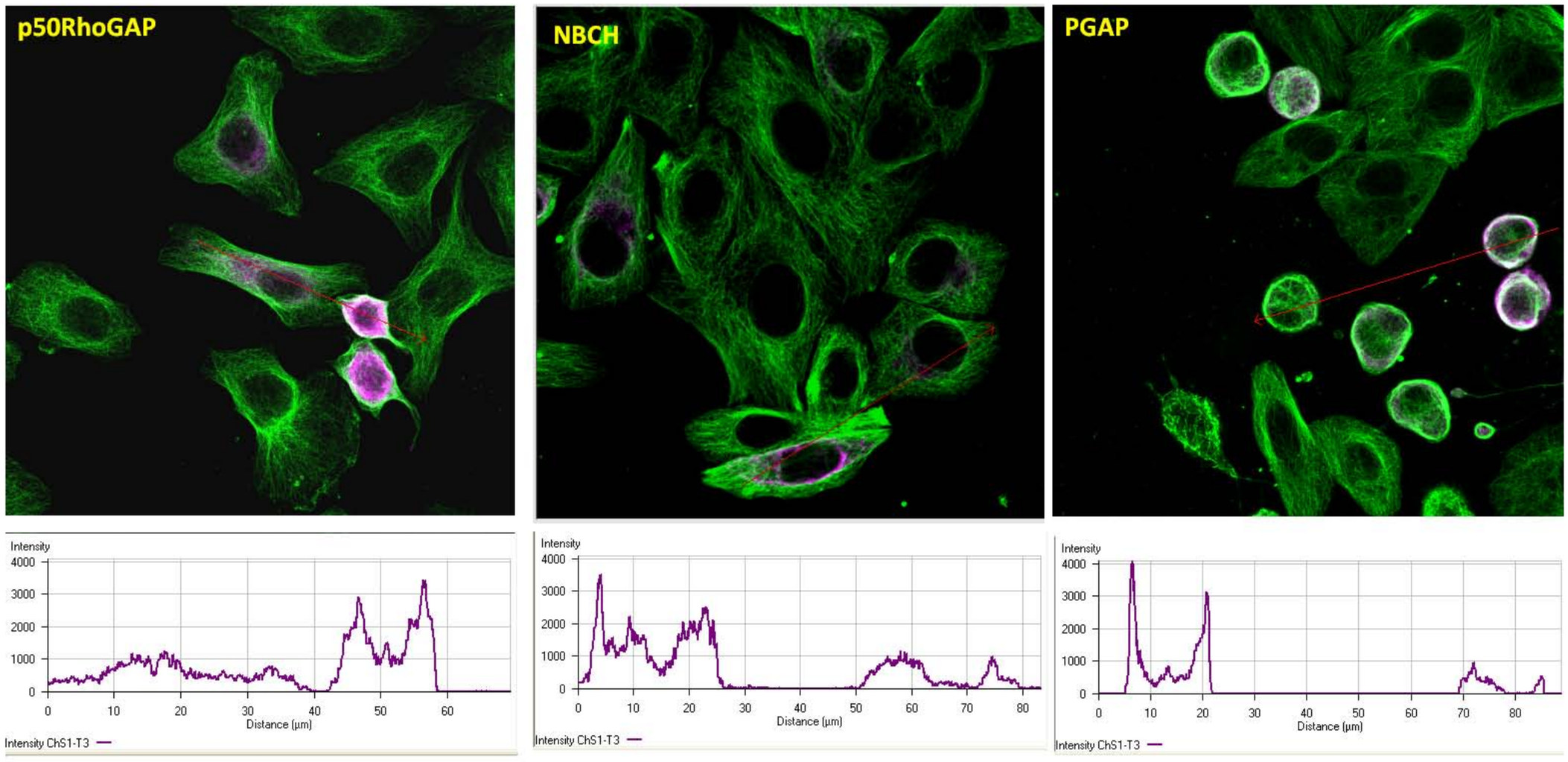
p50RhoGAP
NBCH
PGAP
Intensity
4000
3000
2000
1000
0
0
10
20
30
40
50
60
70
80
Distance (µm)
Intensity ChS1-T3

Figure S3

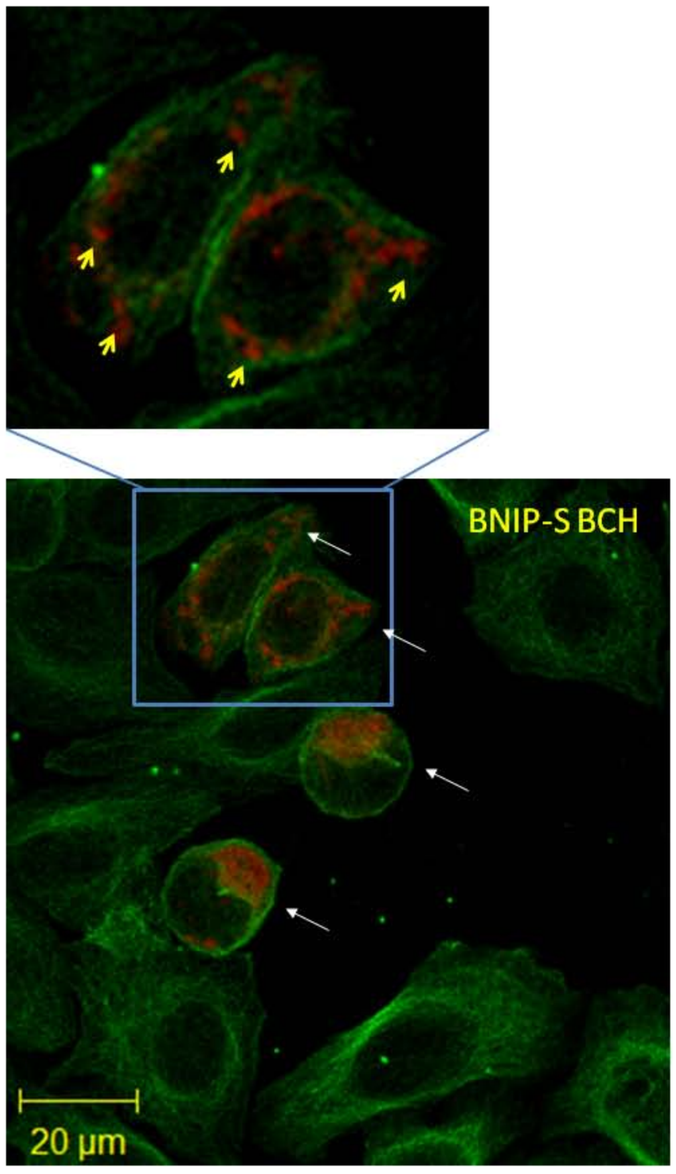

Figure S4

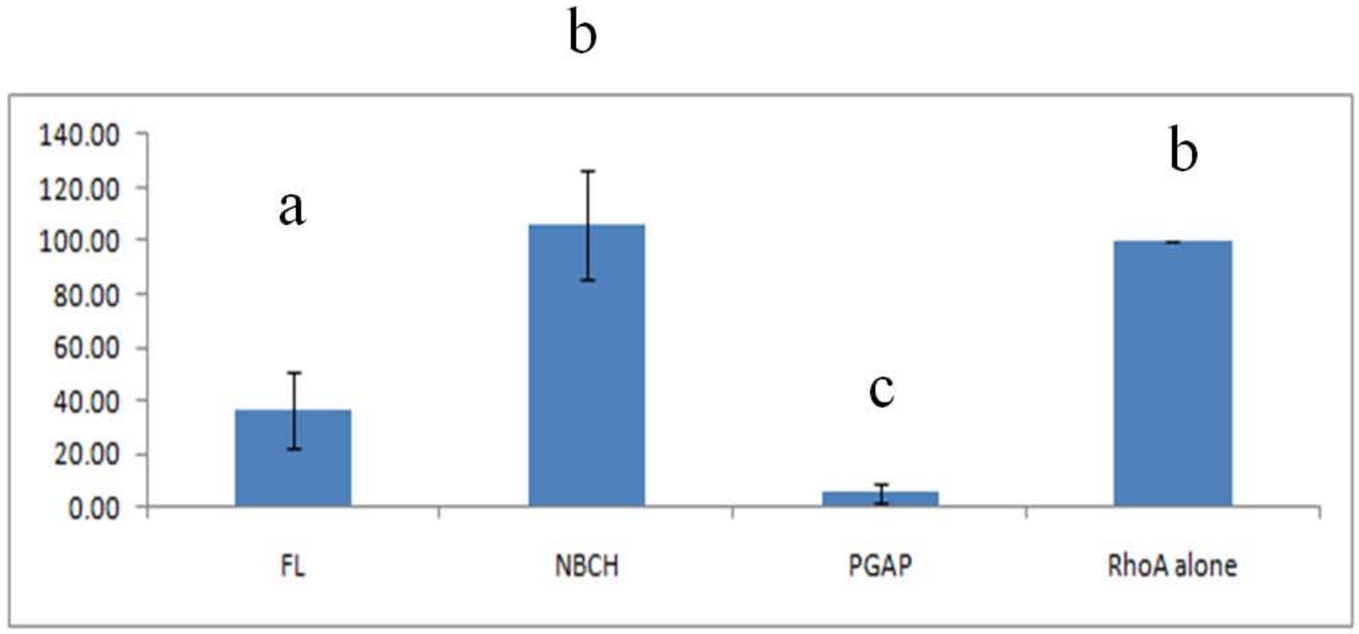
b
140.00
120.00
100.00
80.00
60.00
40.00
20.00
0.00
a
c
b
FL
NBCH
PGAP
RhoA alone

Figure S5

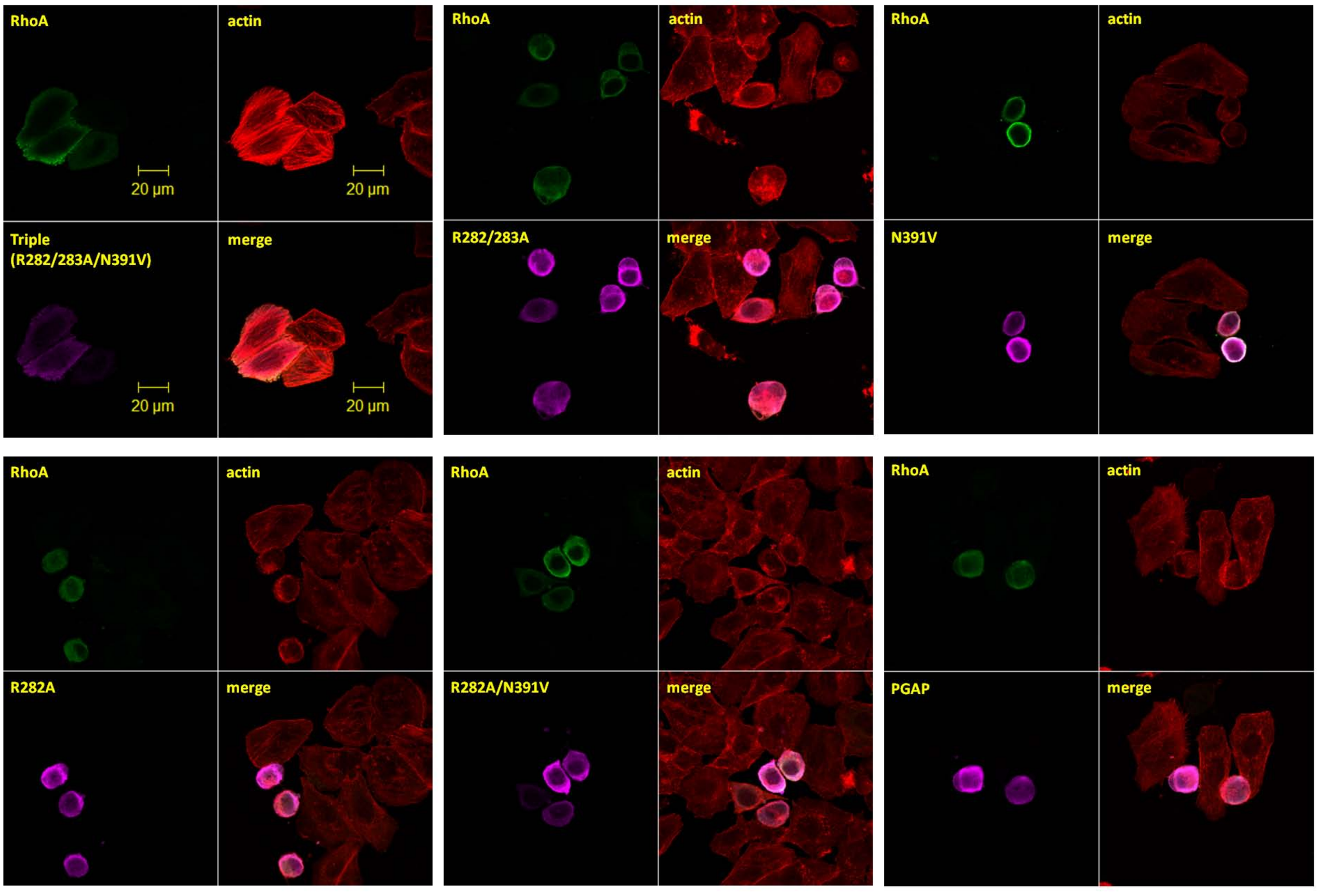
RhoA
actin
20 μm
20 μm
Triple
(R282/283A/N391V)
merge
20 μm
20 μm
RhoA
actin
R282/283A
merge
RhoA
actin
N391V
merge
RhoA
actin
R282A
merge
RhoA
actin
R282A/N391V
merge
RhoA
actin
PGAP
merge

Figure S6

A

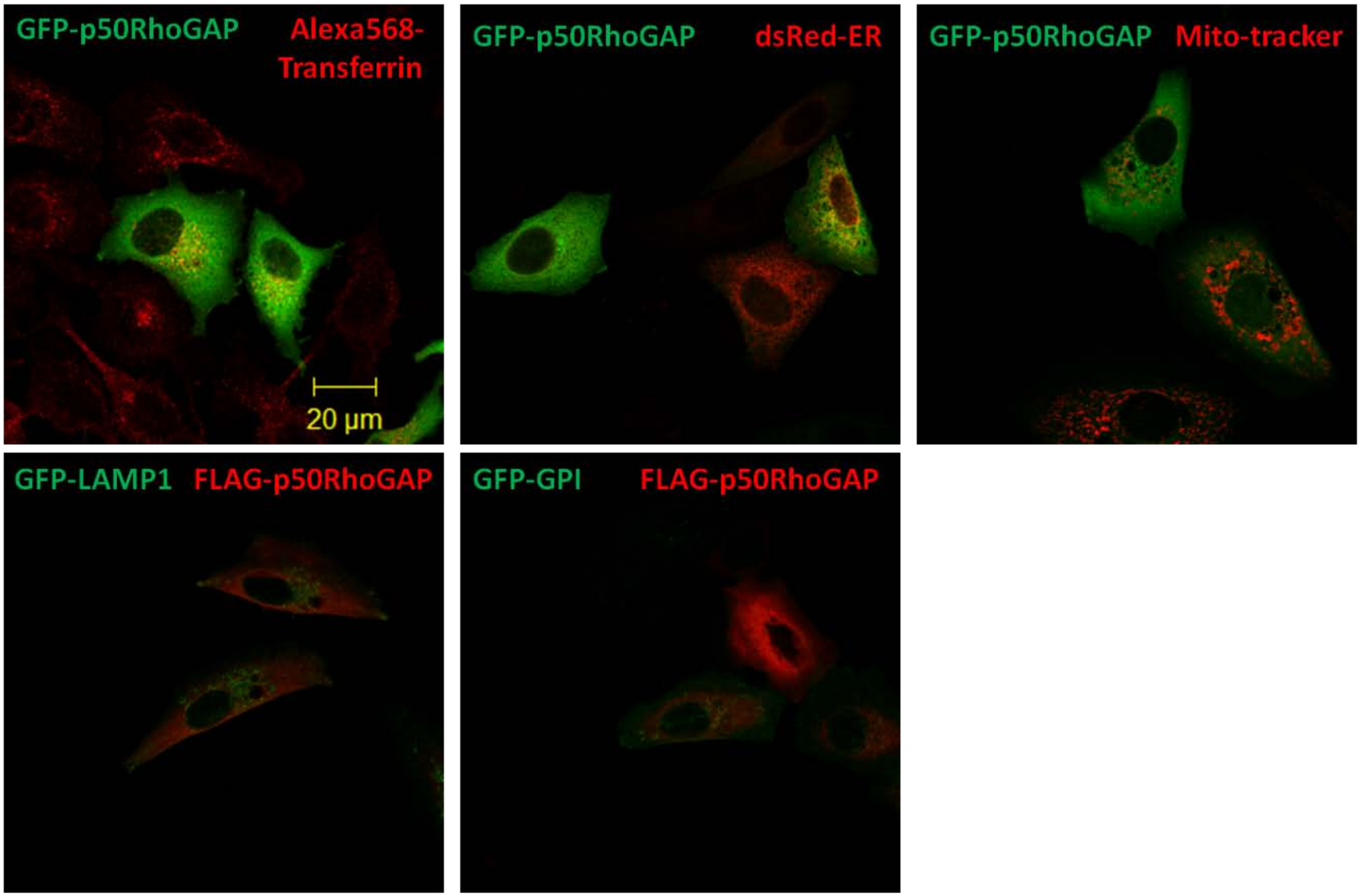
GFP-p50RhoGAP
Alexa568-Transferrin
20 μm
GFP-p50RhoGAP
dsRed-ER
GFP-p50RhoGAP
Mito-tracker
GFP-LAMP1
FLAG-p50RhoGAP
GFP-GPI
FLAG-p50RhoGAP

Figure S6

B

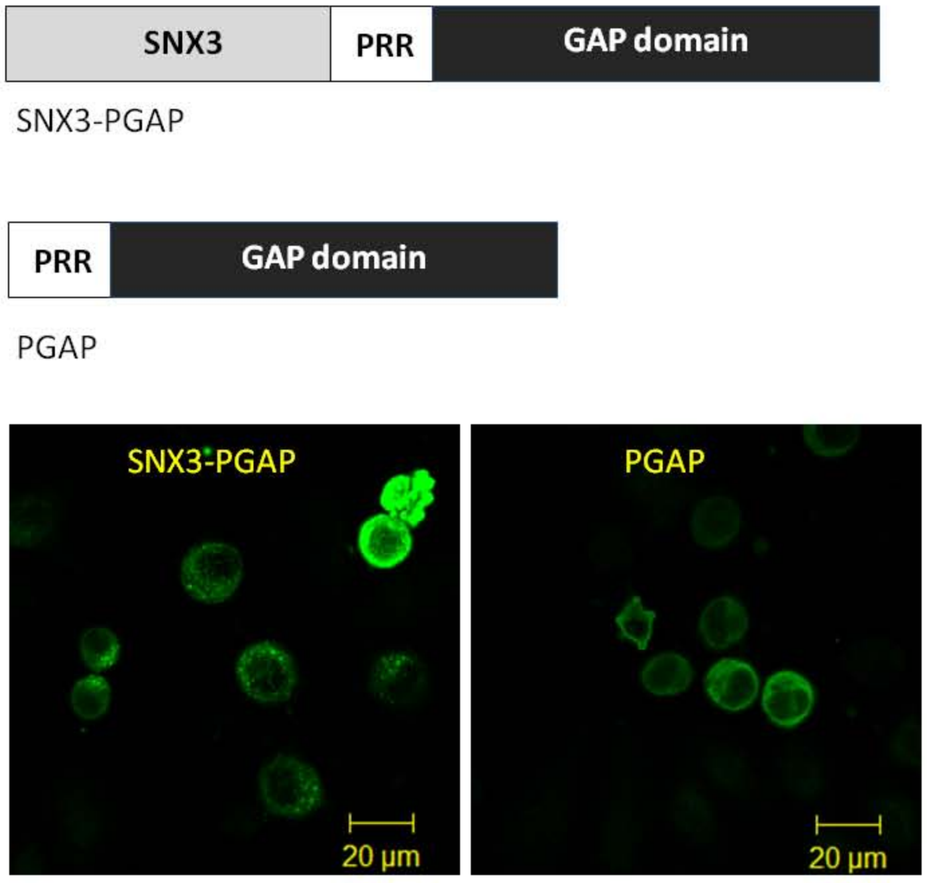
SNX3
PRR
GAP domain
SNX3-PGAP
PRR
GAP domain
PGAP
SNX3-PGAP
20 μm
PGAP
20 μm

C

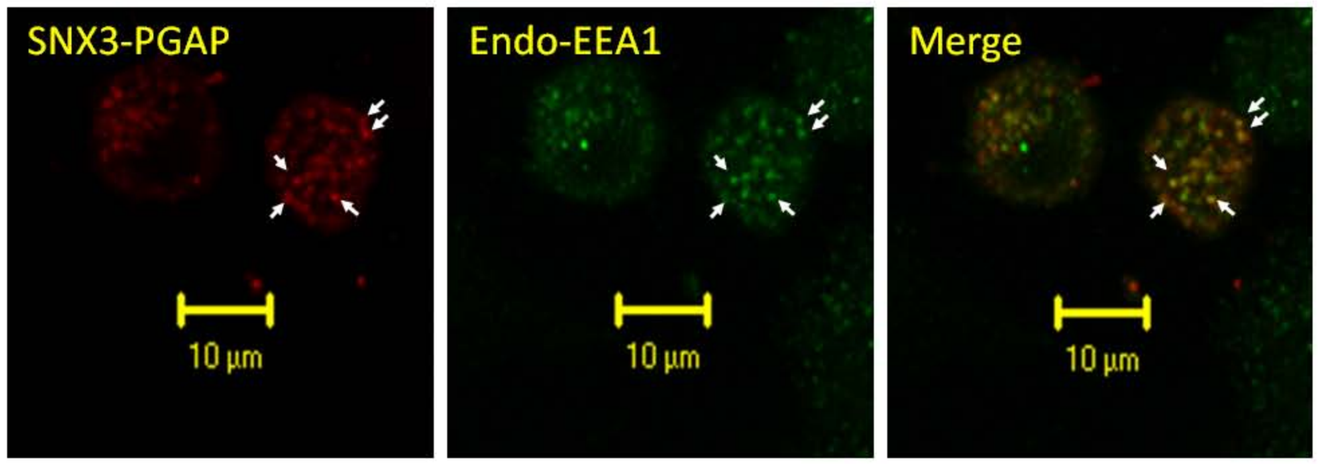
SNX3-PGAP
10 μm
Endo-EEA1
10 μm
Merge
10 μm

Figure S7

A

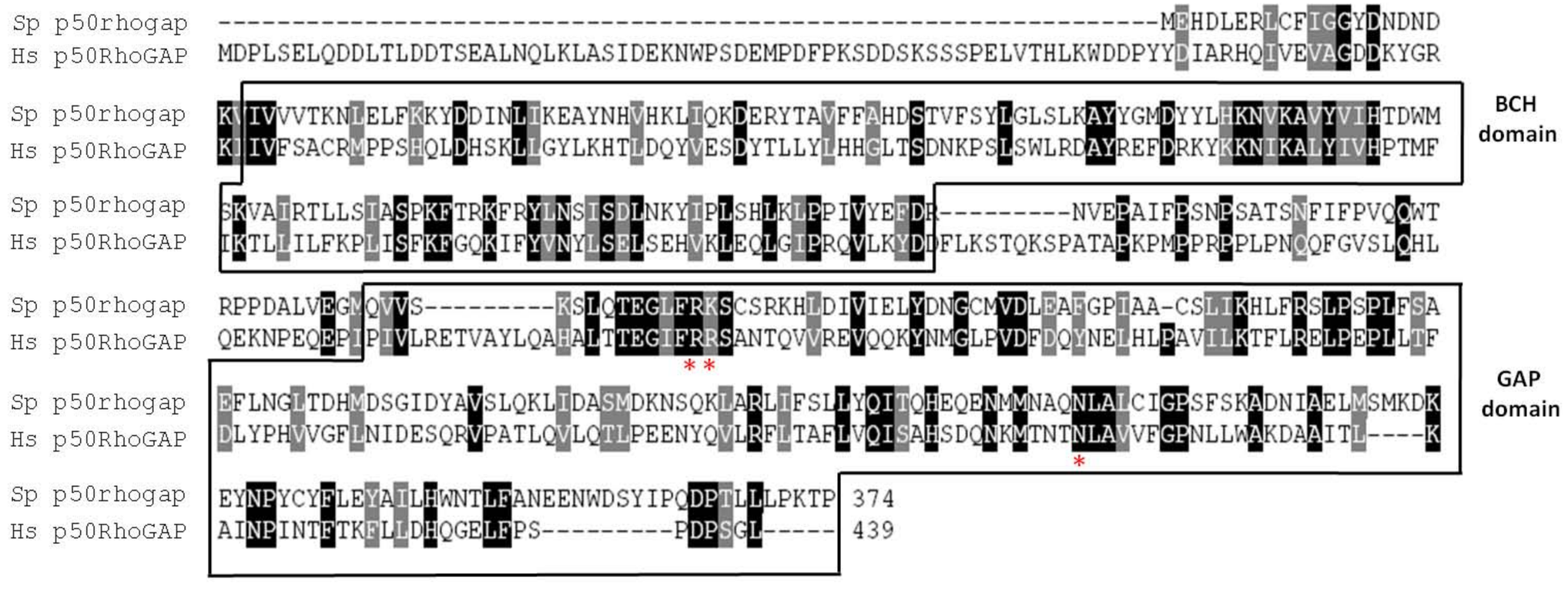
Sp p50rhogap
Hs p50RhoGAP
MDPLSELQDDLTLDDTSEALNQLKLASIDEKNWPSDEMPDFPKSDDSKSSSPELVTHLKWDDPYYDIARHQIVEVAGDDKYGR
BCH domain
RPPDALVEGMQVVS
QEKNPEQEPIPIVLRETVAYLQAHALTTEGIFRRSANTQVVREVQQKYNMGLPVDFDQYNELHLPAVILKTFLRELPEPLLTF
GAP domain
EFLNGLTDHMDSGIDYAVSLQKLIDASMDKNSQKLARLIFSLLYQITQHEQENMMNAQNLALCIGPSFSKADNIAELMSMKDK
DLYPHVVGFLNIDESQRVPATLQVLQTLPEENYQVLRFLTAFLVQISAHSDQNKMTNTNLAVVFGPNLLWAKDAAITL----K
EYNPYCYFLEYAILHWNTLFANEENWDSYIPQDPTLLLPKTP 374
AINPINTFTKFLLDHQGELFPS---------PDPSGL----- 439

B

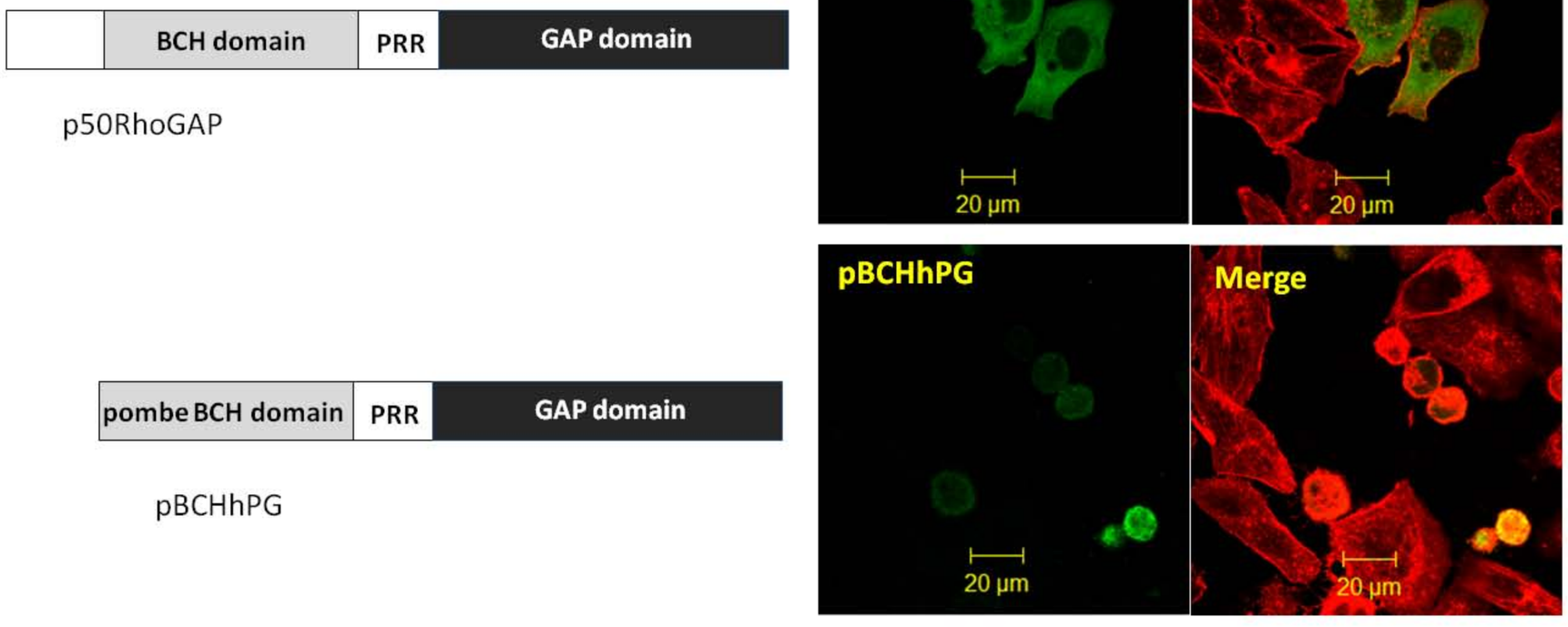
BCH domain
PRR
GAP domain
p50RhoGAP
pombe BCH domain
PRR
GAP domain
pBCHhPG
p50RhoGAP
Merge
pBCHhPG
Merge
20 µm
20 µm
20 µm
20 µm

Figure S7

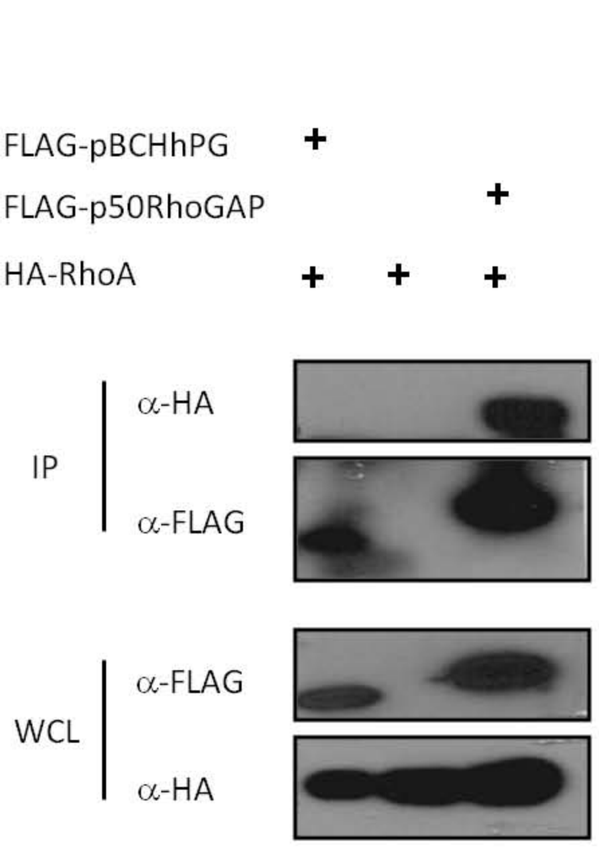
C
FLAG-pBCHhPG +
FLAG-p50RhoGAP +
HA-RhoA + + +
IP
α-HA
α-FLAG
WCL
α-FLAG
α-HA

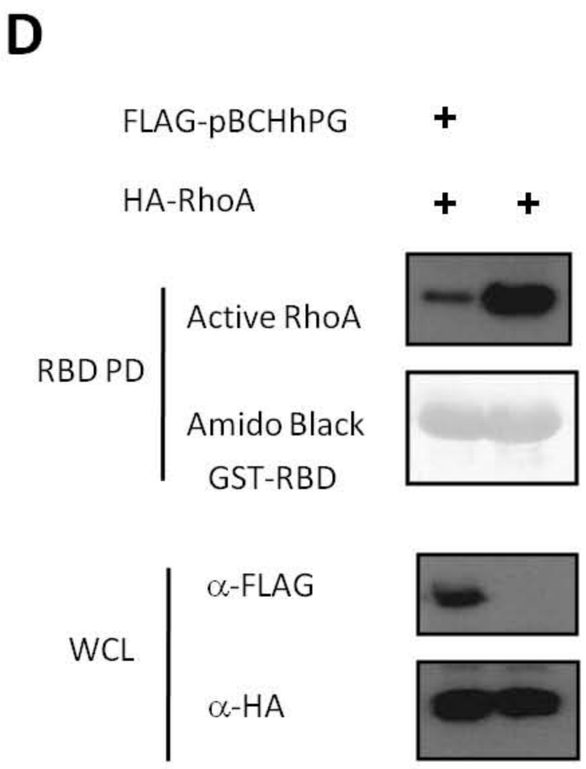
D
FLAG-pBCHhPG +
HA-RhoA + +
RBD PD
Active RhoA
Amido Black
GST-RBD
WCL
α-FLAG
α-HA

Figure S8

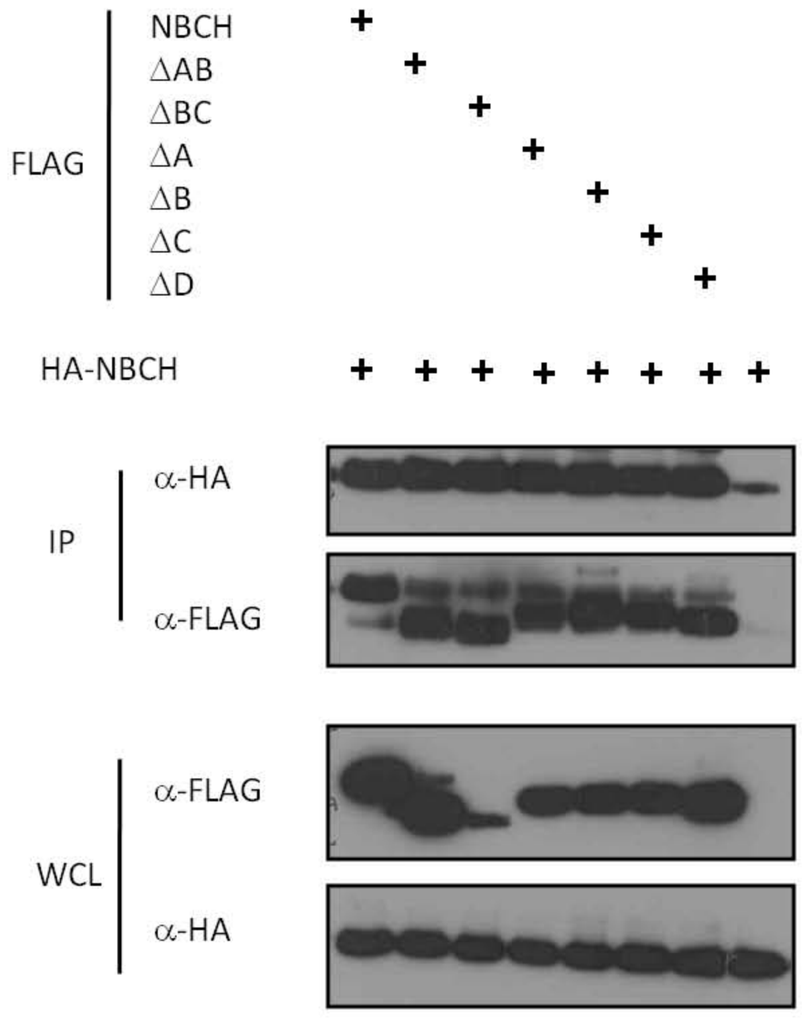

Figure S9

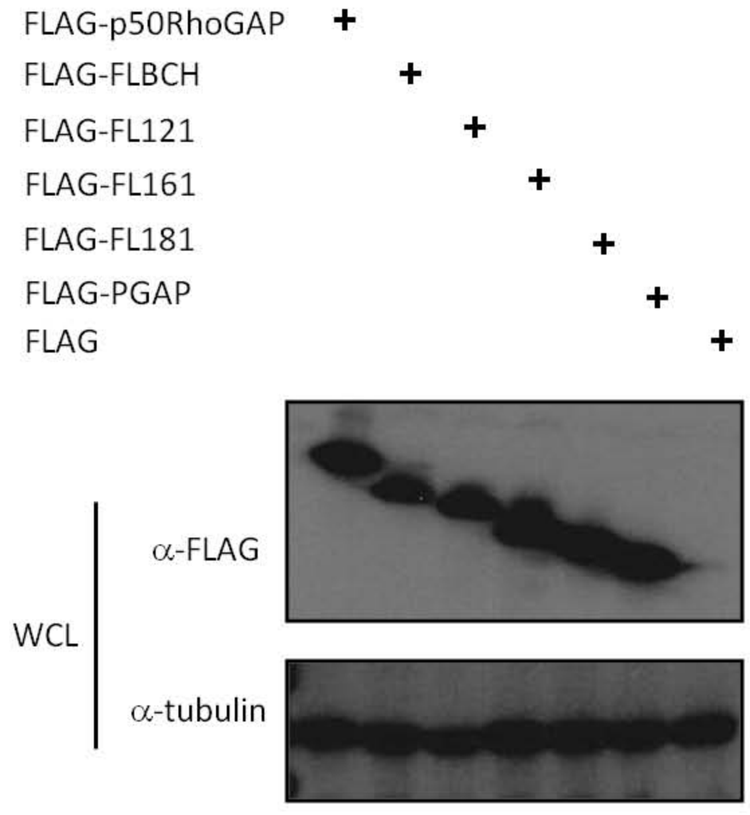
FLAG-p50RhoGAP
FLAG-FLBCH
FLAG-FL121
FLAG-FL161
FLAG-FL181
FLAG-PGAP
FLAG
WCL
α-FLAG
α-tubulin

Figure S10

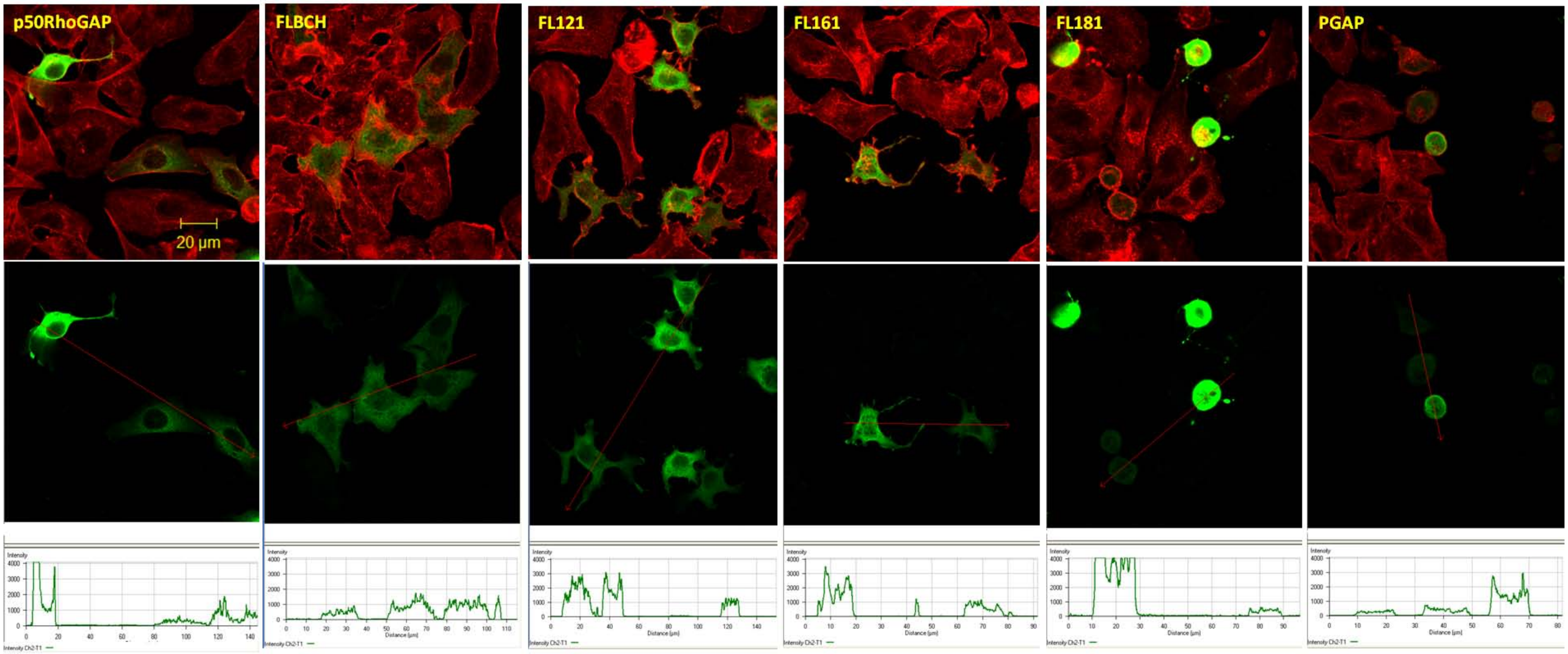
p50RhoGAP
FLBCH
FL121
FL161
FL181
PGAP
20 µm
Intensity
Distance (µm)
Intensity Ch2-T1

Figure S11

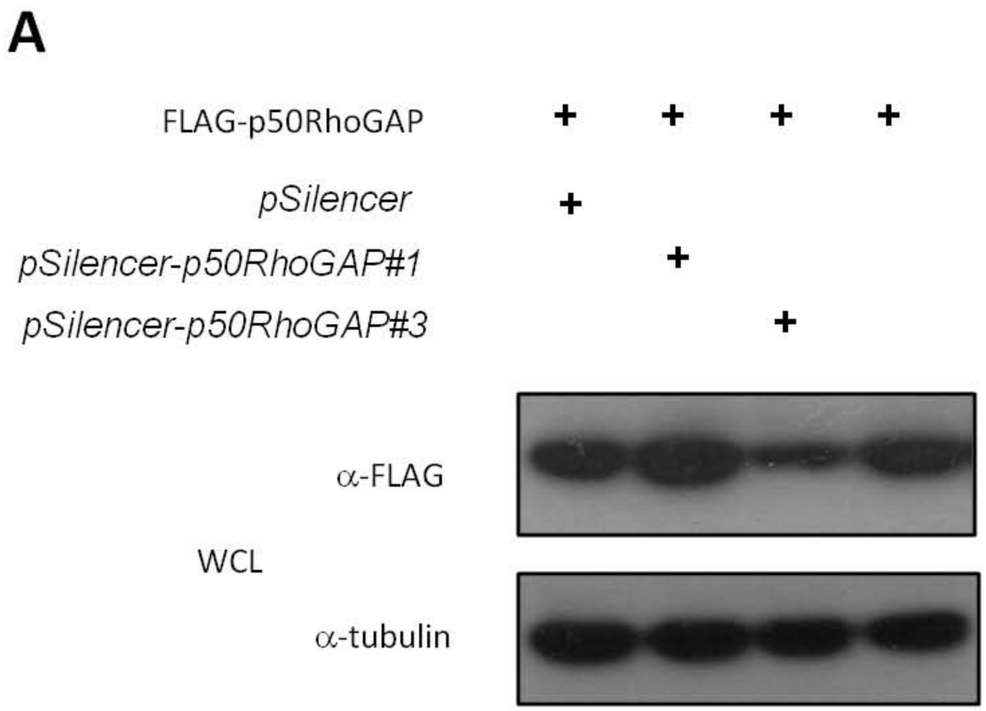
A
FLAG-p50RhoGAP + + + +
pSilencer +
pSilencer-p50RhoGAP#1 +
pSilencer-p50RhoGAP#3 +
α-FLAG
WCL
α-tubulin

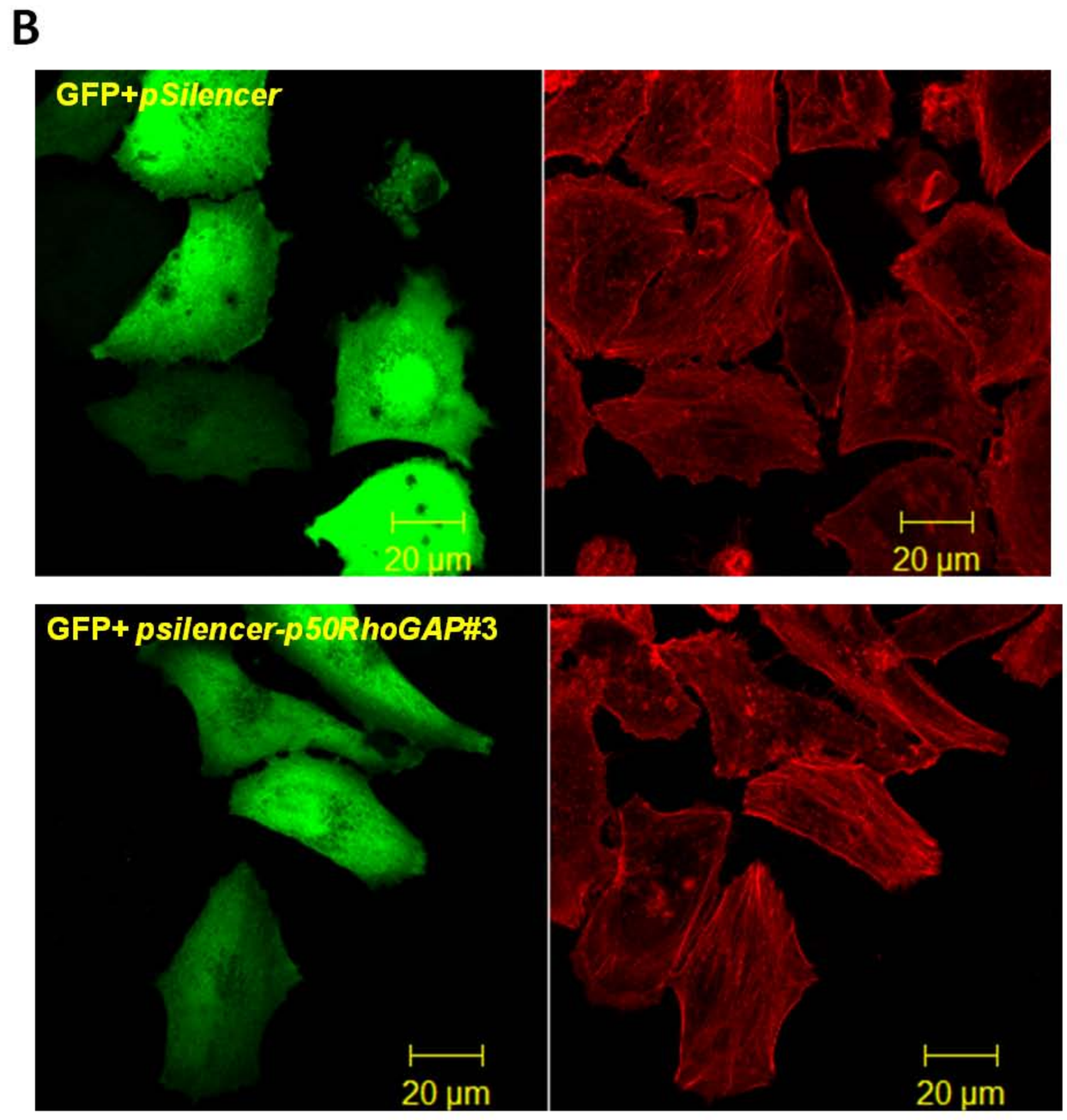
B
GFP+pSilencer
20 μm
20 μm
GFP+ psilencer-p50RhoGAP#3
20 μm
20 μm

Figure S12

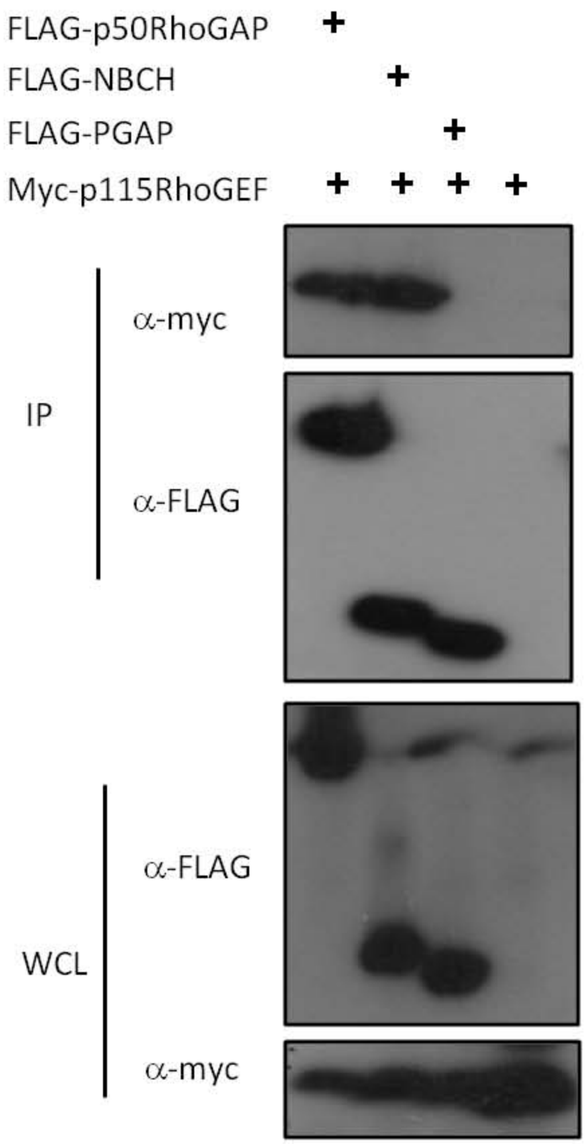
FLAG-p50RhoGAP +
FLAG-NBCH +
FLAG-PGAP +
Myc-p115RhoGEF + + + +
IP
α-myc
α-FLAG
WCL
α-FLAG
α-myc